

## IN VITRO METABOLISM OF ISOLIQURITIGENIN BY HUMAN LIVER MICROSOMES

Jian Guo, Dongting Liu, Dejan Nikolic, Dongwei Zhu, John M. Pezzuto, and  
Richard B. van Breemen

Department of Medicinal Chemistry and Pharmacognosy, University of Illinois College of  
Pharmacy, Chicago, IL (J.G., D.L., D.N., D.Z., R.B.v.B)

School of Pharmacy, University of Hawaii at Hilo, HI (J.M.P.)

Running title: Metabolism of isoliquiritigenin

Address correspondence to:

Richard B. van Breemen

Department of Medicinal Chemistry and Pharmacognosy

University of Illinois College of Pharmacy

833 S. Wood St., Chicago, IL 60612-7231.

E-mail: [breemen@uic.edu](mailto:breemen@uic.edu)

TEL: 312-996-9353

FAX: 312-996-9353

Number of text pages including references: 23

Number of figures: 6

Number of references: 38

Number of words in abstract: 169 words

Number of words in introduction: 308 words

Number of words in discussion: 800 words

Abbreviations:

LC-MS-MS: liquid chromatography-tandem mass spectrometry

HLM: human liver microsomes

M1: liquiritigenin

M2: 2',4,4',5'-tetrahydroxychalcone

M3: 3',4,4'-trihydroxyaurone

M4: 2',3,4,4'-tetrahydroxychalcone

M5: 2',4,4'-trihydroxydihydrochalcone

M6: (*Z*)-6,4'-dihydroxyaurone

M7: (*E*)-6,4'-dihydroxyaurone

SOD: superoxide dismutase

## Abstract

Isoliquiritigenin (2',4',4'-trihydroxychalcone), a chalcone found in licorice root and other plants, has shown potent anti-tumor, antioxidant and phytoestrogenic activity *in vitro*. In preparation for *in vivo* studies, the metabolism of isoliquiritigenin by human liver microsomes was investigated, and seven phase 1 metabolites were identified. In addition to aromatic hydroxylation that occurred on the A or B ring to form 2',4,4',5'-tetrahydroxychalcone or butein, respectively, reduction of the carbon-carbon double bond of an  $\alpha,\beta$ -unsaturated ketone and cyclization occurred to form 2',4,4'-trihydroxydihydrochalcone and (Z/E)-6,4'-dihydroxyaurone. All metabolites were characterized and identified by using liquid chromatography-tandem mass spectrometry with comparison to authenticated compounds. Finally, monoclonal antibody inhibitors of specific human cytochrome P450 enzymes and recombinant human P450 enzymes were used to identify the enzymes responsible for the formation of the major monooxygenated metabolites, and P450 2C19 was found to be a significant enzyme in the formation of butein from isoliquiritigenin, which also has anticancer activity. Cytochrome P450s, reactive oxygen species and peroxidases can all contribute to the formation of (Z/E)-6,4'-dihydroxyaurone in human liver microsomes.

## Introduction

Isoliquiritigenin is a chalcone found in licorice (*Glycyrrhiza uralensis*), shallots (*Allium ascalonicum*), *Sinofranchetia chinensis*, *Dalbergia odorifera*, and soybeans (*Glycine max* L.) (Cao, et al., 2004; Kape, et al., 1992; Kong, et al., 2000; Pan, et al., 2000; Ramadan, et al., 2000) and has been found to have antioxidant (Vaya, et al., 1997), anti-inflammatory (Chan, et al., 1998), phytoestrogenic (Maggiolini, et al., 2002; Tamir, et al., 2001), and tyrosinase inhibitory properties (Nerya, et al., 2004). Isoliquiritigenin also exhibits significant anticancer activity such as induction of cell cycle arrest and up-regulation of p21 expression in a lung cancer cell line (li, et al., 2004), suppression of pulmonary metastasis of mouse renal cell carcinoma through activation of the immune system (Yamazaki, et al., 2002), and induction of apoptosis in human gastric cancer cells (Ma, et al., 2001). As a chemopreventive agent, isoliquiritigenin has been shown *in vivo* to prevent colon and mammary cancer in several rat carcinogenesis models (Baba, et al., 2002; Wattenberg, et al., 1994). Another mechanism of chemoprevention by isoliquiritigenin is induction of phase 2 enzymes, such as quinone reductase, that protect cells against reactive, toxic, and potentially carcinogenic species (Ross et al., 2000; Cuendet et al., 2006).

Although isoliquiritigenin is a promising anti-tumor agent, there has been no comprehensive evaluation of its phase 1 metabolism. Since phase 1 metabolism might introduce hydroxyl groups to form products with new pharmacological activities, we identified 7 metabolites, M1-M7, of isoliquiritigenin formed by pooled human liver microsomes using liquid chromatography-tandem mass spectrometry (LC-MS-MS) and comparison to standards. Several previously unreported metabolites formed through

unusual pathways were identified. The cytochrome P450 enzymes involved in the generation of the most abundant hydroxylated metabolites of isoliquiritigenin were identified, and their relative contributions to the formation of major each metabolite was determined using monoclonal antibody inhibitors of specific P450 enzymes and corresponding recombinant human P450 enzymes.

## Methods

### Materials

Isoliquiritigenin was isolated from *Glycyrrhiza uralensis* and purified by using semi-preparative HPLC. The purity was determined to be >98% based on analysis using HPLC with UV absorbance detection and liquid chromatograph-mass spectrometry (LC-MS). Authentic standards of the metabolites, butein and sulfarein, were purchased from Indofine (Hillsborough, NJ). All other chemicals were purchased from Sigma-Aldrich (St. Louis, MO). HPLC-grade solvents were purchased from Fisher Scientific (Pittsburgh, PA).

Pooled human liver microsomes were purchased from In Vitro Technologies (Baltimore, MD). The cytochrome P450 content of the microsomes was 0.17 nmol of P450/mg of protein. Anti-P450 1A1, 1A2, 2A6, 2B6, 2C8, 2C9, 2C19, 2D6, 2E1, and 3A4 monoclonal antibodies were obtained from Dr. Harry Gelboin of the National Institutes of Health (Bethesda, MD). Microsomes from baculovirus-infected insect cells containing human cytochrome P450 reductase and human cytochrome *b*<sub>5</sub> with cDNA-expressed human P450 1A1, 1A2, 2B6, 2C8, 2C9, 2C9\*1, 2C18, 2C19, 2D6, 2E1, 3A4,

and 3A5 (0.5 nmol cytochrome P450 in 0.5 mL) were purchased from Gentest (Woburn, MA) and In Vitro Technologies.

#### *Synthesis of 4,2',4'-trihydroxydihydrochalcone (M5)*

Formic acid (0.02 mL) was added dropwise to a mixture of isoliquiritigenin (60 mg, 0.2 mmol), triethylamine (0.1 mL), and 10% Pd/C (0.2 g) (195 mg, 1.59 mmol) in tetrahydrofuran (5 mL) at room temperature, and the reaction mixture was stirred at room temperature for 1 h. The palladium was removed by filtration, and the solvent was evaporated to give a light yellow oil which was purified by flash chromatography on silica gel using chloroform/methanol (30:1, v/v) as the eluent, yielding a light yellow oil (49 mg, 89%) that was identified spectroscopically as 4,2',4'-trihydroxydihydrochalcone as follows: mp < 20 °C. <sup>1</sup>H-NMR (CD<sub>3</sub>OD, 400 MHz) δ 2.91 (t, 2H, *J* = 7.2 Hz, β-H), 3.17 (t, 2H, *J* = 7.2 Hz, α-H), 6.26 (d, 1H, *J* = 2.0 Hz, 3'-H), 6.34 (dd, 1H, *J* = 2.0 Hz, *J* = 8.8 Hz, 5'-H), 6.72 (d, 2H, *J* = 8.4 Hz, 3,5-H), 6.86 (d, 2H, *J* = 8.4 Hz, 2,6-H), 7.7 (d, 1H, *J* = 2.0 Hz, 6'-H); <sup>13</sup>C-NMR (CD<sub>3</sub>OD, 400 Hz) δ 29.61 (β-C), 39.52 (α-C), 102.28 (3'-C), 107.77 (5'-C), 112.60 (1'-C), 114.82 (3,5-C), 128.99 (2,6-C), 131.80 (1-C), 132.36 (6'-C), 155.30 (4-C), 165.03 (2'-C), 168.84 (4'-C), 204.16 (C=O). MS (negative ion electrospray) *m/z* 257.1 ([M-H]<sup>-</sup>, 15%), 151.1 (100%), 139.0, 109.0, 107.0; high resolution negative ion electrospray mass spectrometry measured for C<sub>15</sub>H<sub>13</sub>O<sub>4</sub>, [M-H]<sup>-</sup> *m/z* 257.0813 (calculated 257.0814, Δ = 3.9 ppm).

#### *Synthesis of 6,4'-dihydroxyaurone (M6 and M7)*

A solution of 6-hydroxy-3-coumaranone (200 mg, 1.33 mmol) and 4-hydroxybenzaldehyde (195 mg, 1.59 mmol) in ethanol (4 mL) was refluxed for 3 h. The reaction was quenched by pouring the mixture into ice-water. After filtration, the solid

product was washed with water and dried, and 6,4'-dihydroxyaurone (300 mg, 88%) was obtained as a yellow powder. The *E/Z* ratio of (*E*)-6,4'-dihydroxyaurone M7 (28.5 %) and (*Z*)-6,4'-dihydroxyaurone M6 (71.5 %) was determined by using LC-MS. After recrystallization from chloroform/methanol, the pure (*Z*)-isomer was obtained, and its configuration was determined by gate-decoupling correlation NMR. <sup>1</sup>H-NMR (CD<sub>3</sub>OD, 400 MHz) δ 6.69 (s, 1H, =CH), 6.74 (m, 2H, 5,7-H), 6.89 (d, 2H, *J*=8.4 Hz, 3',5'-H), 7.62 (d, 1H, *J*=8.4 Hz, 4-H), 7.81 (d, 2H, *J*=8.4 Hz, 2',6'-H); <sup>13</sup>C-NMR (CD<sub>3</sub>OD, 400 Hz) δ 97.61 (=CH), 112.24 (4 or 5-CH), 112.38 (5 or 4-CH), 115.18 (2',4'-CH), 123.22, 125.04 (7-CH), 132.86 (3',5'-CH), 145.91, 159.14, 166.46, 168.02, 182.52 (3-CO). MS (negative ion electrospray) *m/z* 252.9 ([M-H]<sup>-</sup>, 100%), 223.9, 207.9, 196.9, 180.9, 134.9, 116.9, 90.9; high resolution negative ion electrospray mass spectrometry measured for C<sub>15</sub>H<sub>9</sub>O<sub>4</sub>, [M-H]<sup>-</sup> *m/z* 253.0499 (calculated 253.0501, Δ = 8.0 ppm).

#### *Microsomal incubations*

Incubations with pooled human liver microsomes contained 0.5 mg/mL of microsomal protein, 10 or 50 μM isoliquiritigenin, and 1 mM NADPH in 50 mM phosphate buffer at pH 7.4 in a total volume of 0.4 mL. In one set of experiments, the effect of NADPH concentration on the formation of isoliquiritigenin metabolism was investigated using NADPH at 0.1, 0.01 and 0.002 mM in addition to 1 mM. The reactions were initiated by addition of NADPH after a 5 min preincubation and were carried out at 37 °C for 40 min. The incubations were terminated by adding 1.6 mL of an ice-cold mixture of acetonitrile/ethanol (1:1, v/v) and chilling the resulting mixture on ice. After centrifugation to remove the precipitated proteins, the supernatant was evaporated to dryness *in vacuo*. Each residue was reconstituted in 150 μL of HPLC mobile phase

immediately prior to analysis using LC-MS. All incubations were carried out at least three times, and the mean values were compared using one-way ANOVA with Tukey test,  $p \leq 0.01$ .

To investigate the effect of superoxide and hydrogen peroxide on the formation of the metabolite aurone, superoxide dismutase (SOD) (200 U/mL), catalase (1000 U/mL), catalase/ $\text{NaN}_3$  (1 mM), or ascorbic acid (1 mM) was used to pretreat the human liver microsomes for 30 min at room temperature before the addition of isoliquiritigenin and NADPH. Alternatively, as inhibitors of peroxidases,  $\text{NaN}_3$  (1 mM) or guaiacol (25 mM) with or without  $\text{H}_2\text{O}_2$  (200  $\mu\text{M}$ ) was included in the pre-incubation mixture. The reaction was initiated by the addition of isoliquiritigenin (10  $\mu\text{M}$ ) with or without 1 mM NADPH.

#### *Inhibition of cytochrome P450 enzymes in human liver microsomes*

To identify the relative contributions of specific cytochrome P450 enzymes in human liver that are responsible for the formation of the monooxygenated metabolite M4, incubations were carried out using human liver microsomes and monoclonal antibodies that selectively inhibit specific cytochrome P450. The protein concentrations of the monoclonal antibodies were determined using the method of Bradford (1976) with bovine serum albumin as a standard. The inhibitory activity of the monoclonal antibodies was verified as described previously (Guo, et al., 2006). Each inhibitory monoclonal antibody (0, 0.2, or 0.4 mg protein/mL) was incubated with human liver microsomes (0.5 mg protein/mL) and 10  $\mu\text{M}$  of individual substrate (phenacetin for P450 1A2, amodiaquine for P450 2C8, tolbutamide for P450 2C9, S-mephenytoin for P450 2C19, dextromethorphan for P450 2D6, chlorzoxazone for P450 2E1, and testosterone

for P450 3A) for 30 min at 37 °C. The results were used to determine the optimal concentrations of antibodies required for maximal inhibition. Addition of 0.4 mg protein/mL of each monoclonal antibody resulted in 90, 85, 80, 100, 90, 90, and 86% inhibition of P450 1A2, 2C8, 2C9, 2C19, 2D6, 2E1, and 3A, respectively. All subsequent incubations contained 10 µM isoliquiritigenin, 0.5 mg/mL of human hepatic microsomal protein, and a monoclonal antibody inhibitor of a specific cytochrome P450 enzyme at a final concentration of 0.4 mg/mL in 50 mM phosphate buffer at pH 7.4. After a 5 min preincubation at 37 °C, the reaction was initiated by the addition of NADPH (1 mM final concentration) in a total incubation volume of 0.4 mL. Control incubations were carried out that contained all components except the inhibitory antibody. The incubations were terminated by the addition of 1.6 mL of ice-cold acetonitrile/ethanol and then analyzed using LC-MS-MS.

#### *Identification of P450 enzymes responsible for metabolism of isoliquiritigenin*

The P450 enzymes involved in the formation of the most abundant monooxygenated isoliquiritigenin metabolites (M3 and M4; Figure 1) were determined using cDNA-expressed human P450 1A1, 1A2, 2B6, 2C8, 2C9, 2C9\*1, 2C18, 2C19, 2D6, 2E1, 3A4, and 3A5. A 10 µM solution of isoliquiritigenin in 200 µL phosphate buffer (pH 7.4) was incubated with 20 pmol of each P450 enzyme and 1 mM NADPH for 10 min at 37 °C. Each incubation was terminated by the addition of 1.6 mL of an ice-cold mixture of acetonitrile/ethanol (1:1, v/v) to precipitate proteins and chilling the mixture on ice. The relative amounts of M3 and M4 formed by each enzyme were determined using LC-MS.

#### *Cyclization of isoliquiritigenin*

To evaluate the potential for isoliquiritigenin to cyclize to a flavonoid when exposed to acid in the stomach, 10  $\mu\text{M}$  isoliquiritigenin was incubated for 1 h at room temperature or 37 °C in either water or 0.05% HCl. Eriodictyol (0.5  $\mu\text{M}$ , final concentration) was spiked into each sample as an internal standard before analysis using LC-MS to determine the amount of cyclization. Alternatively, the decrease in absorbance of isoliquiritigenin was measured at 372 nm as it cyclized to a flavonone.

#### *LC-MS and LC-MS-MS*

During LC-MS-MS, reversed phase HPLC separations were carried out using a Zorbax SB 2.1 x 100 mm C<sub>18</sub> column (3.5  $\mu\text{m}$  particle size) with a Waters (Milford, MA) 2690 solvent delivery system. The mobile phase consisted of a linear gradient from 0.05% formic acid in water to methanol as follows: 20-70% methanol over 25 min and 70-95% methanol over the next 10 min at a flow rate of 0.2 mL/min. The column temperature was 30 °C, and the autosampler was maintained at 4 °C. Accurate mass measurements and product ion tandem mass spectra were acquired using negative ion electrospray with a Micromass (Manchester, UK) Q-TOF-2 hybrid quadrupole/time-of-flight mass spectrometer. Tandem mass spectra were acquired using collision-induced dissociation with argon as the collision gas at a pressure of  $2.0 \times 10^{-5}$  mBar and a collision energy of 25 eV.

Quantitative analysis of isoliquiritigenin was carried out using LC-MS with negative ion electrospray and selected ion monitoring on an Agilent (Palo Alto, CA) G1946A quadrupole mass spectrometer and Model 1100 HPLC system equipped with a photodiode array UV detector. In addition, UV spectra were acquired during these analyses over the range 200 to 400 nm. The HPLC solvent system was identical to that

used during the LC-MS-MS separation described above. During LC-MS with selected ion monitoring, the deprotonated molecules of isoliquiritigenin and the internal standard eriodictyol were detected at  $m/z$  255.1 and 287.1, respectively. The  $[M-H]^-$  ions of dihydrochalcone (M5), aurone (M6 and M7), an aurone metabolite M3, and the monohydroxylated isoliquiritigenin metabolites M2 and M4 were monitored at  $m/z$  257.1, 253.1, 269.1, and 271.1, respectively.

## Results

### *Identification of isoliquiritigenin metabolites*

The total ion chromatogram and computer-reconstructed selected ion chromatograms for the negative ion electrospray LC-MS analysis of an incubation of isoliquiritigenin with pooled human liver microsomes are shown in Figure 1. Four major (M1, M3, M4, M6) and three minor (M2, M5, M7) metabolites (based on abundances during LC-MS, Figure 1) were detected as their deprotonated molecules. As indicated in the tandem mass spectra shown in Figure 2, the major MS fragmentation pathway for isoliquiritigenin was a retro Diels-Alder reaction, producing  $A^-$  and  $B^-$  ions of  $m/z$  135 and 119, respectively. Retro Diels-Alder fragmentation is typical of chalcones during collision-induced dissociation and provides helpful information for the structure determination of corresponding metabolites (Nikolic et al., 2005).

Eluting at a retention time of 15.3 min during LC-MS (see Figure 1), M1 was the most abundant derivative of isoliquiritigenin (retention time 19.9 min). The exact mass of M1 was identical to isoliquiritigenin ( $[M-H]^-$   $m/z$  255.066), matching the theoretical composition of  $C_{15}H_{12}O_4$  ( $\Delta = 0.8$  ppm). The negative ion electrospray product ion

tandem mass spectra of M1 and isoliquiritigenin are shown in Figure 2 and are also indistinguishable. The UV absorbance spectra of M1 and isoliquiritigenin were recorded during LC-UV-MS and showed absorbance maxima of 274 and 372 nm, respectively. This difference indicates the loss of  $\pi$ -bond conjugation in the structure of M1. Therefore, M1 was probably a cyclized product of the chalcone isoliquiritigenin, and this was confirmed by comparison with authentic 4,4'-dihydroxyflavanone (liquiritigenin). Since M1 was also observed in control incubations in which isoliquiritigenin was incubated without human liver microsomes or NADPH, the formation of liquiritigenin did not depend upon enzymatic catalysis. The rate of cyclization of isoliquiritigenin in 0.05% HCl at 37 °C was then investigated and was found to be identical to that at pH 7.4 and 37 °C (data not shown). However, temperature did affect cyclization, since the yield of M1 was ~3-fold greater at 37 °C compared to room temperature (data not shown). These data suggest that cyclization of isoliquiritigenin to M1 is temperature dependant and that stomach acid will not catalyze this process.

A minor monooxygenated metabolite eluting at 16.6 min (Figure 1), isoliquiritigenin metabolite M2 formed a deprotonated molecule of  $m/z$  271.0584, which corresponded to an elemental composition of  $C_{15}H_{11}O_5$  ( $\Delta = 8.5$  ppm). The abundant mass product ions of  $m/z$  151 ( $A^-$ ) and  $m/z$  119 ( $B^-$ ) formed during tandem mass spectrometry with CID indicated that the new oxygen of M2 was introduced into the A-ring (see Figure 2). However, hydroxylation could have occurred at the 3', 5', or 6' position of the A-ring. Based on the comparison of retention time and tandem mass spectra with a reference compound, M2 was identified as 2',4,4',5'-tetrahydroxychalcone, confirming that hydroxylation took place at the 5'

position of the A-ring. It should be noted that the fragment ion of  $m/z$  123, formed by elimination of CO from  $m/z$  151 (see Figure 2), distinguished M2 as containing a *para*-hydroxylated A-ring as reported by Zhang and Brodbelt (2003).

Metabolite M3, eluting at a 17.9 min during LC-MS (Figure 1), formed a deprotonated molecule of  $m/z$  269.0454. Exact mass measurement indicated an elemental composition of  $C_{15}H_9O_5$  ( $< 1.5$  ppm). Therefore, M3 was formed from isoliquiritigenin by introduction of one oxygen atom accompanied by a loss of two hydrogen atoms. The formation of an abundant product ion of  $m/z$  135 instead of  $m/z$  119 during LC-MS-MS (Figure 3) indicated that a hydroxyl group had been introduced into the B-ring. Analysis of the UV spectrum showed that the absorption maximum of M3 was at 398 nm with a 26 nm bathochromic shift in Band I, which corresponds to the B-ring (Markham, 1980). This absorbance wavelength is too long for most classes of flavanoids except for aurones, which contain a five-membered ring (Mabry, et al., 1970). The most abundant product ion of  $m/z$  133.04 in the negative ion tandem mass spectrum of M3 was formed from the B-ring and is a characteristic fragment ion of aurones (Figure 3) (Kesari, et al., 2004). The tentative identification of M3 as 3',4,4'-trihydroxyaurone (sulfuretin) was confirmed by comparison with an authentic standard.

The second most abundant isoliquiritigenin metabolite M4 eluted at 17.8 min during LC-MS (Figure 1) and formed a deprotonated molecule of  $m/z$  271.0580, which was within -9.8 ppm of the formula  $C_{15}H_{11}O_5$ . The base peak of  $m/z$  135 in the tandem mass spectrum indicated that oxidation occurred on the B-ring (Figure 2). The UV absorbance maximum of M4 was measured at 382 nm, which is only 10 nm higher than

that of isoliquiritigenin, indicating that hydroxylation occurred at the 3-position of B-ring to form 2',3,4,4'-tetrahydrochalcone (butein) (Markham, 1980). This assignment was confirmed by comparison with the authentic standard.

The minor metabolite M5 eluted at 18.7 min (Figure 1). Accurate mass measurement of the deprotonated molecule of M5 indicated a molecular formula of  $C_{15}H_{13}O_4$  (measured  $m/z$  257.0814;  $\Delta = 0.1$  ppm), which contained 2H more than isoliquiritigenin. The decreased intensity of UV absorbance at 254 nm and 274 nm compared to isoliquiritigenin indicated a loss of conjugation between the two aromatic rings. The base peak of  $m/z$  151 ( $A^-$ ) and the ion of  $m/z$  107 ( $B^-$ ) in the product ion tandem mass spectrum indicated that the  $\alpha,\beta$ -unsaturated double bond had been eliminated through reduction (Figure 3). The structure of M5 was confirmed as 2',4,4'-trihydroxydihydrochalcone (davidigenin) by comparison of the UV spectrum, tandem mass spectrum and co-elution during LC-MS with a standard. As indicated in Figure 1, M5 was formed in only trace amounts relative to abundant products such as M1 and M4. Like M1, M5 was also detected in control incubation and did not require enzymes for its formation.

During LC-MS, metabolites M6 and M7 of isoliquiritigenin were detected eluting at 19.5 and 20.2 min, respectively. Accurate mass measurements provided values of  $m/z$  253.0520 and 253.0479, which were within -7.6 and -8.6 ppm of the theoretical formula  $C_{15}H_9O_4$ , respectively. The UV spectra of M6 and M7 shared an absorbance maximum at 398 nm. This bathochromic shift compared to the absorbance maximum of 372 nm for isoliquiritigenin and the characteristic product ions of  $m/z$  135 ( $A^-$ ) and 117 ( $B^-$ ) indicated that M6 and M7 were both aurone (Figure 3). Moreover, the similarity of

the product ion tandem mass spectra of M6 and M7 (Figure 3) suggested that these two metabolites are *E* and *Z* stereoisomers of 6,4'-dihydroxyaurone. By comparison to synthetic standards that had been analyzed using FT-NMR, M6 was determined to be (*Z*)-6,4'-dihydroxyaurone and M7 was (*E*)-6,4'-dihydroxyaurone.

During the LC-MS analysis of metabolites of isoliquiritigenin (Figure 1), *cis*- and *trans*-6,4'-dihydroxyaurone (M6 and M7) were formed in control incubations that did not contain NADPH. Therefore, additional incubations of isoliquiritigenin with human liver microsomes were carried out in which the concentration of NADPH was varied. The formation of metabolites M3 and M4 was NADPH-dependent, and the yield of these metabolites decreased as the concentration of NADPH was reduced. For example, at 100, 10, and 2  $\mu$ M NADPH, the yield of M3 was 74, 15, and 0%, respectively, relative to the yield at 1 mM NADPH. Similarly, the yield of M4 was 57, 9, and 0% when the concentration of NADPH was 100, 10 and 2  $\mu$ M, respectively. However, at  $\leq 10$   $\mu$ M NADPH, the formation of M6 remained constant at ~50% of the yield at 1 mM NADPH. At NADPH concentrations less than 10  $\mu$ M, no other metabolites were detected. These results indicated that cytochrome P450 enzymes were responsible for the formation of M3 and M4 and only partially contributed to the generation of M6 and M7.

Additional incubations of isoliquiritigenin with human liver microsomes were carried out that included SOD, catalase, ascorbic acid, sodium azide, or guaiacol but not NADPH, and the results are shown in Figure 4. Since M6 and M7 are stereoisomers and the relative amount of M6 is much greater than that of M7, only the yield of M6 was measured while investigating the factors responsible for the formation of aurone. Pre-treating human liver microsomes with SOD decreased the formation of M6 by 70%, and

addition of catalase reduced the formation of M6 by 58%. Co-incubation of human liver microsomes with  $\text{NaN}_3$ , a mechanism-based inhibitor of peroxidase, resulted in a 40% decrease of M6 formation compared to incubation with human liver microsomes alone. Guaiacol, a competitive inhibitor of peroxidase in the presence of  $\text{H}_2\text{O}_2$  (Doerge, et al., 1997), decreased the formation of M6 by 95% and 50% with or without added  $\text{H}_2\text{O}_2$ , respectively. The addition of a free radical scavenger and inhibitor of peroxidase, ascorbic acid, significantly inhibited the formation of M6 by 93%. These results indicate that  $\text{H}_2\text{O}_2$ , superoxide and peroxidase contribute to the formation of M6 and M7.

To determine which enzymes were responsible for the formation of M3 and M4, isoliquiritigenin was incubated with individual recombinant human P450 enzymes and NADPH, and the results are shown in Figure 5. These recombinant enzyme data suggested that P450 2C19, 2E1, and 2C9 contribute most to the formation of M3, although trace metabolite formation was detected for other enzymes. The most abundant phase 1 metabolite of isoliquiritigenin, M4, was formed primarily by P450 2C19. Confirmation that P450 2C19 was the primary enzyme catalyzing the formation of M4 was obtained using human liver microsomes that had been treated with monoclonal antibodies to inhibit each of 9 different major enzymes (Figure 6). No specific cytochrome P450 enzymes were identified that might contribute to the formation of M6 or M7, instead, all of the enzymes tested appeared to contribute slightly.

M4 is the major monooxygenated metabolite of isoliquiritigenin. To determine the contribution of each P450 enzyme towards M4 formation, the incubation of isoliquiritigenin and human liver microsomes were carried out with each of 9 different monoclonal antibodies that inhibit the major P450 enzymes. The results of these

inhibition assays showed that the presence of monoclonal antibody against P450 2C19 resulted in a 66% decrease of M4 formation (Figure 6). This result is consistent with that obtained in the experiments using recombinant P450 enzymes.

## Discussion

Chalcones contain two aromatic rings connected by an unsaturated carbon chain and are the intermediate precursors for all flavonoid compounds. Hydroxychalcones are distributed throughout the plant kingdom and can form flavonoids and isoflavonoids (Otani, et al., 1994; Sabzevari, et al., 2004). Hydroxychalcones with phenolic groups on both the A- and B-rings are more cytotoxic and more effective as cancer therapeutic agents than those containing a hydroxyl group only on the A-ring (Sabzevari, et al., 2004). Therefore, some of the hydroxylated metabolites of isoliquiritigenin might be more effective than isoliquiritigenin itself as antioxidants and chemopreventive agents. For example, the catechol butein (2',4',3,4-tetrahydroxychalcone; M4) is a more potent antioxidant, electron donor and hydrogen donor than isoliquiritigenin (2,4,4"-trihydroxychalcone) due to the extra hydroxyl group (Nerya, et al., 2004). Although the apoptosis induction activity of butein (M4) is weaker than that of isoliquiritigenin, butein has been reported to inhibit cell proliferation and induce apoptosis in B16 melanoma cells by down-regulating expression of the anti-apoptotic proteins Bcl-2 (Iwashita, et al., 2000). Butein is also a potent antioxidant, probably due to the presence of the catechol substructure (Vaya, et al., 2003). Butein is one of the seven metabolites or derivatives of isoliquiritigenin formed during incubation with human liver microsomes that are shown in Scheme 1.

Since M1 was observed in control incubations that did not contain human liver microsomes or NADPH, it may be considered a degradation product as well as a metabolite of isoliquiritigenin. The cyclization of chalcones to the corresponding flavonones, such as the formation of 4,4'-dihydroxyflavone from isoliquiritigenin, is well known (Nikolic, et al., 2005). Like isoliquiritigenin and its metabolite butein (M4), M1 has also been reported to have chemoprevention activity. For example, M1 has been shown to exhibit cytotoxic activity toward five human cancer cell lines *in vitro* (Falcao, et al., 2005).

The aurone metabolite sulfuretin (M3) and a related aurone, 3'4'-dihydroxyaurone, have been reported to have chemoprevention activities. For example, Park, et al. (2004) found that sulfuretin has antimutagenic properties and can prevent genotoxicity caused by certain electrophilic intermediates. By preventing DNA strand scission and inhibiting sphingosine kinase, 3'4'-dihydroxyaurone can inhibit tumor growth (French, et al., 2003; Huang, et al., 1998).

The formation of metabolites M3 and M4 was dependent on the concentration of NADPH, and neither product could be detected when the initial NADPH concentration was < 10  $\mu$ M. Since liver microsomes were also required for the formation of M3 and M4, the generation of these isoliquiritigenin metabolites was probably catalyzed by cytochrome P450 enzymes. Incubation of isoliquiritigenin with c-DNA expressed human P450s or hepatic microsomes treated with monoclonal antibody inhibitors of specific human P450 enzymes showed that P450 2C19 and 2E1 are major isozymes contributing to M3 formation, and that M4 formation was catalyzed primarily by P450 2C19.

Stevens *et al.* (2003) reported the superoxide anion-mediated formation of aurone from chalcone during an investigation of peroxynitrite-mediated LDL oxidation. In our studies, the formation of stereoisomers of 6,4'-dihydroxyaurone, M6 and M7, was also found to depend on superoxide, since co-incubation of isoliquiritigenin with SOD, which converts superoxide to H<sub>2</sub>O<sub>2</sub> (O'Brien, 2000), inhibited their formation. Since interconversion of reactive oxygen species can occur, incubation of isoliquiritigenin with catalase, which converts H<sub>2</sub>O<sub>2</sub> to O<sub>2</sub> and H<sub>2</sub>O (Komatsu, et al., 2002), also reduced the formation of M6 and M7, and this effect was reversed by treatment with NaN<sub>3</sub>, an inhibitor of catalase. The role of reactive oxygen species in the formation of M6 and M7 from isoliquiritigenin was confirmed by inhibition of this process by ascorbic acid (a free radical scavenger and peroxidase inhibitor). In addition, 6,4'-dihydroxyaurone (M6 and/or M7) are known to be peroxidase-catalysed oxidation products of isoliquiritigenin (Rathmell, 1972). In our studies, inhibitory effects of NaN<sub>3</sub> (an inhibitor of peroxidase) and guaiacol (a competitive inhibitor of the peroxidase/H<sub>2</sub>O<sub>2</sub> system) on M6 formation were observed. Since hydroxyl free radical and superoxide anion are reactive oxygen species produced in P450/NADPH catalytic reactions (Karuzina and Archakov, 1994), their production can catalyze the cyclization of isoliquiritigenin to form M6 and M7 which is consistent with our data that liver microsomes contributed to the formation of ~50% of M6 and M7. Therefore, both P450 enzymes and peroxidases contributed to the cyclization of isoliquiritigenin to form the aurones M6 and M7. A proposed free radical catalyzed mechanism of formation of M6 and M7 from isoliquiritigenin via a quinone intermediate is shown in Scheme 2.

During this investigation, seven microsomal metabolites and derivatives of isoliquiritigenin were identified using LC-MS-MS with comparison to standards. Some of these derivatives were cyclization products such as M1, M3, M6, and M7, and others were monohydroxylation products such as M2, M3 (also a cyclization product) and M4. Since many of these derivatives have already been reported to have chemoprevention activity, metabolites of isoliquiritigenin might contribute to the anticancer effects of this chemopreventive agent.

## References

- Baba M, Asano R, Takigami I, Takahashi T, Ohmura M, Okada Y, Sugimoto H, Arika T, Nishino H and Okuyama T (2002) Studies on cancer chemoprevention by traditional folk medicines XXV. Inhibitory effect of isoliquiritigenin on azoxymethane-induced murine colon aberrant crypt focus formation and carcinogenesis. *Biol Pharm Bull* **25**:247-250.
- Bradford MM (1976) A rapid and sensitive method for the quantitation of microgram quantities of protein utilizing the principle of protein-dye binding. *Anal Biochem* **72**:248-254.
- Cao Y, Wang Y, Ji C and Ye J (2004) Determination of liquiritigenin and isoliquiritigenin in *Glycyrrhiza uralensis* and its medicinal preparations by capillary electrophoresis with electrochemical detection. *J Chromatogr A* **1042**:203-209.
- Chan SC, Chang YS, Wang JP, Chen SC and Kuo SC (1998) Three new flavonoids and antiallergic, anti-inflammatory constituents from the heartwood of *Dalbergia odorifera*. *Planta Med* **64**:153-158.
- Cuendet M, Oteham CP, Moon RC and Pezzuto JM (2006) Quinone reductase induction as a biomarker for cancer chemoprevention. *J Nat Prod* **69**:460-463.
- Doerge DR, Divi RL and Churchwell MI (1997) Identification of the colored guaiacol oxidation product produced by peroxidases. *Anal Biochem* **250**:10-17.

Falcao MJ, Pouliquem YB, Lima MA, Gramosa NV, Costa-Lotufo LV, Militao GC, Pessoa C, de Moraes MO and Silveira ER (2005) Cytotoxic flavonoids from *Platymiscium floribundum*. *J Nat Prod* **68**:423-426.

French KJ, Schrecengost RS, Lee BD, Zhuang Y, Smith SN, Eberly JL, Yun JK and Smith CD (2003) Discovery and evaluation of inhibitors of human sphingosine kinase. *Cancer Res* **63**:5962-5969.

Guo J, Nikolic D, Chadwick LR, Pauli GF and van Breemen RB (2006) Identification of human hepatic cytochrome P450 enzymes involved in the metabolism of 8-prenylnaringenin and isoxanthohumol from hops (*Humulus lupulus* L.). *Drug Metab Dispos* **34**:1152-1159.

Huang L, Wall ME, Wani MC, Navarro H, Santisuk T, Reutrakul V, Seo EK, Farnsworth NR and Kinghorn AD (1998) New compounds with DNA strand-scission activity from the combined leaf and stem of *Uvaria hamiltonii*. *J Nat Prod* **61**:446-450.

li T, Satomi Y, Katoh D, Shimada J, Baba M, Okuyama T, Nishino H and Kitamura N (2004) Induction of cell cycle arrest and p21 (CIP1/WAF1) expression in human lung cancer cells by isoliquiritigenin. *Cancer Lett* **207**:27-35.

Iwashita K, Kobori M, Yamaki K and Tsushida T (2000) Flavonoids inhibit cell growth and induce apoptosis in B16 melanoma 4A5 cells. *Biosci Biotechnol Biochem* **64**:1813-1820.

- Kape R, Parniske M, Brandt S and Werner D (1992) Isoliquiritigenin, a strong nod gene- and glyceollin resistance-inducing flavonoid from soybean root exudate. *Appl Environ Microbiol* **58**:1705-1710.
- Karuzina II and Archakov AI (1994) The oxidative inactivation of cytochrome P450 in monooxygenase reactions. *Free Radic Biol Med* **16**:73-97.
- Kesari AN, Gupta RK and Watal G (2004) Two aurone glycosides from heartwood of *Pterocarpus santalinus*. *Phytochemistry* **65**:3125-3129.
- Komatsu T, Yamazaki H, Nakajima M and Yokoi T (2002) Identification of catalase in human livers as a factor that enhances phenytoin dihydroxy metabolite formation by human liver microsomes. *Biochem Pharmacol* **63**:2081-2090.
- Kong LD, Zhang Y, Pan X, Tan RX and Cheng CH (2000) Inhibition of xanthine oxidase by liquiritigenin and isoliquiritigenin isolated from *Sinofranchetia chinensis*. *Cell Mol Life Sci* **57**:500-505.
- Ma J, Fu NY, Pang DB, Wu WY and Xu AL (2001) Apoptosis induced by isoliquiritigenin in human gastric cancer MGC-803 cells. *Planta Med* **67**:754-757.
- Mabry TJ, Markham KR and Thomas MB (1970) *The systematic identification of flavonoids*. Springer-Verlag, New York, Berlin.
- Maggiolini M, Statti G, Vivacqua A, Gabriele S, Rago V, Loizzo M, Menichini F and Amdo S (2002) Estrogenic and antiproliferative activities of isoliquiritigenin in MCF7 breast cancer cells. *J Steroid Biochem Mol Biol* **82**:315-322.

Markham KR (1980) *Techniques of flavonoids identification*. Academic Press, New York.

Nerya O, Musa R, Khatib S, Tamir S and Vaya J (2004) Chalcones as potent tyrosinase inhibitors: the effect of hydroxyl positions and numbers. *Phytochemistry* **65**:1389-1395.

Nikolic D, Li Y, Chadwick LR, Pauli GF and van Breemen RB (2005) Metabolism of xanthohumol and isoxanthohumol, prenylated flavonoids from hops (*Humulus lupulus* L.), by human liver microsomes. *J Mass Spectrom* **40**:289-299.

O'Brien PJ (2000) Peroxidases. *Chem Biol Interact* **129**:113-139.

Otani K, Takahashi T, Furuya T and Ayabe S (1994) Licodione synthase, a cytochrome P450 monooxygenase catalyzing 2-hydroxylation of 5-deoxyflavanone, in cultured *Glycyrrhiza echinata* L. cells. *Plant Physiol* **105**:1427-1432.

Pan X, Kong LD, Zhang Y, Cheng CH and Tan RX (2000) In vitro inhibition of rat monoamine oxidase by liquiritigenin and isoliquiritigenin isolated from *Sinofranchetia chinensis*. *Acta Pharmacol Sin* **21**:949-953.

Park KY, Jung GO, Lee KT, Choi J, Choi MY, Kim GT, Jung HJ and Park HJ (2004) Antimutagenic activity of flavonoids from the heartwood of *Rhus verniciflua*. *J Ethnopharmacol* **90**:73-79.

Ramadan MA, Kamel MS, Ohtani K, Kasai R and Yamasaki K (2000) Minor phenolics from *Crinum bulbispermum* bulbs. *Phytochemistry* **54**:891-896.

- Rathmell WG, Bendall DB (1972) The peroxidase-catalysed oxidation of a chalcone and its possible physiological significance. *Biochem. J.* **127**:125-132
- Ross D, Kepa JK, Winski SL, Beall HD, Anwar A and Siegel D (2000) NAD(P)H:quinone oxidoreductase 1 (NQO1): chemoprotection, bioactivation, gene regulation and genetic polymorphisms. *Chem Biol Interact* **129**:77-97.
- Sabzevari O, Galati G, Moridani MY, Siraki A and O'Brien PJ (2004) Molecular cytotoxic mechanisms of anticancer hydroxychalcones. *Chem Biol Interact* **148**:57-67.
- Stevens JF, Miranda CL, Frei B and Buhler DR (2003) Inhibition of peroxynitrite-mediated LDL oxidation by prenylated flavonoids: the  $\alpha,\beta$ -unsaturated keto functionality of 2'-hydroxychalcones as a novel antioxidant pharmacophore. *Chem Res Toxicol* **16**:1277-1286.
- Tamir S, Eizenberg M, Somjen D, Izrael S and Vaya J (2001) Estrogen-like activity of glabrene and other constituents isolated from licorice root. *J Steroid Biochem Mol Biol* **78**:291-298.
- Vaya J, Belinky PA and Aviram M (1997) Antioxidant constituents from licorice roots: isolation, structure elucidation and antioxidative capacity toward LDL oxidation. *Free Radic Biol Med* **23**:302-313.
- Vaya J, Mahmood S, Goldblum A, Aviram M, Volkova N, Shaalan A, Musa R and Tamir S (2003) Inhibition of LDL oxidation by flavonoids in relation to their structure and calculated enthalpy. *Phytochemistry* **62**:89-99.

Wattenberg LW, Coccia JB and Galbraith AR (1994) Inhibition of carcinogen-induced pulmonary and mammary carcinogenesis by chalcone administered subsequent to carcinogen exposure. *Cancer Lett* **83**:165-169.

Yamazaki S, Morita T, Endo H, Hamamoto T, Baba M, Joichi Y, Kaneko S, Okada Y, Okuyama T, Nishino H and Tokue A (2002) Isoliquiritigenin suppresses pulmonary metastasis of mouse renal cell carcinoma. *Cancer Lett* **183**:23-30.

Zhang J and Brodbelt JS (2003) Structural characterization and isomer differentiation of chalcones by electrospray ionization tandem mass spectrometry. *J Mass Spectrom* **38**:555-572.

## Footnotes

This research was supported by grant P01 CA48112 from the National Cancer Institute.

## Legends for Figures

Figure 1. *Computer-reconstructed mass chromatograms for the negative ion electrospray LC-MS analysis of metabolites of isoliquiritigenin.* Metabolites M1, M2, M3, M4, M5, M6, and M7 were identified as liquiritigenin, 2',4,4',5'-tetrahydroxychalcone, sulfuretin, butein, davidigenin, *trans*-6,4'-dihydroxyaurone, and *cis*-6,4'-dihydroxyaurone, respectively. Note that the control incubation which contained human liver microsomes (HLM) but no NADPH showed the formation of *cis*- and *trans*-6,4'-dihydroxyaurone (M6 and M7).

Figure 2. *Negative ion electrospray CID tandem mass spectra of the deprotonated molecules of A) isoliquiritigenin; B) M1; C) M2; and D) M4.*

Figure 3. *Negative ion electrospray CID tandem mass spectra of the deprotonated moleculeS of A) M3; B) M5; C) M6; and D) M7.*

Figure 4. *Effects of NADPH, sodium azide, SOD, catalase, ascorbic acid, and guaiacol on the formation of M6 by pooled HLM.* Isoliquiritigenin (10  $\mu$ M) was incubated with HLM (0.5 mg/mL) and 1 mM NADPH, NaN<sub>3</sub> (1 mM), SOD (200 U/mL), catalase (1000 U/mL), catalase/NaN<sub>3</sub> (1 mM), ascorbic acid (1 mM), or guaiacol (25 mM) at 37 °C for 30 min. The reaction mixtures were analyzed by using LC-MS.

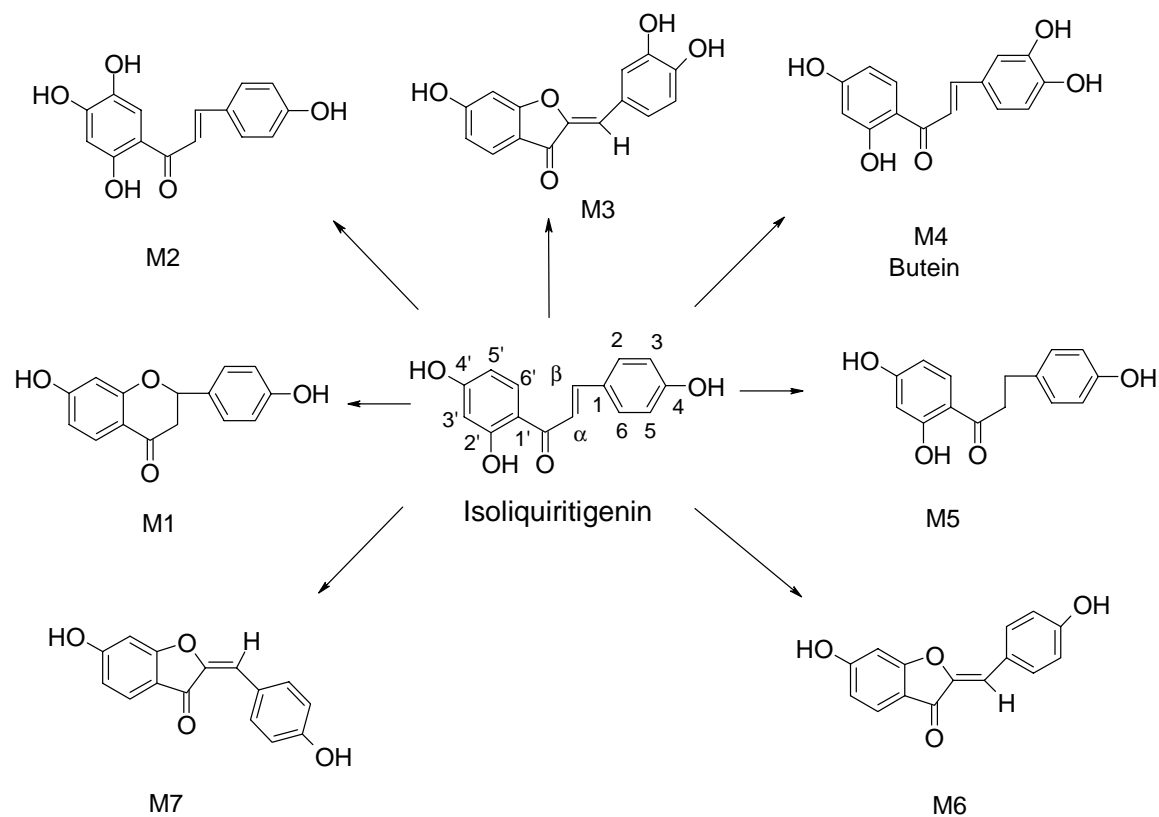
\*Significant difference between HLM incubations with and without NADPH. \*\*Significant difference between incubations containing catalase and catalase/NaN<sub>3</sub> determined using one-way ANOVA with the Tukey test,  $p \leq 0.01$  (Mean  $\pm$  Std Error;  $N = 3$ ).

Figure 5. *P450 isozymes involved in the formation of A) M3; and B) M4.* Isoliquiritigenin (10  $\mu$ M) was incubated with expressed human P450 enzymes (0.5 mg/mL) at 37 °C for 10 min in the presence of the NADPH (1 mM). TE and TSE were media used in the incubations. The reaction mixtures were analyzed by using LC-MS (Mean  $\pm$  Std Error;  $N = 3$ ).

Figure 6. *Confirmation of P450 2C19 as the enzyme responsible for the formation of isoliquiritigenin metabolite M4.* Monoclonal antibodies that inhibit specifically one cytochrome P450 enzyme were incubated with isoliquiritigenin (10  $\mu$ M) and human liver microsomes (HLM) (0.5 mg/mL) at 37 °C for 30 min. Incubation with HLM without antibody was used as a control. The formation of M4 was suppressed only when P450 2C19 was inhibited by a specific monoclonal antibody. Therefore, P450 2C19 catalyzes the formation of M4 from isoliquiritigenin.

\*Denotes significant inhibition compared to the control (HLM only) and determined using one-way ANOVA with the Tukey test,  $p \leq 0.01$  (Mean  $\pm$  Std Error;  $N = 3$ ).

Scheme 1. *Proposed metabolic pathways for human liver phase 1 metabolism of isoliquiritigenin*



Scheme 2. A proposed free radical catalyzed mechanism of formation of metabolites M6 and M7 involving a quinone intermediate

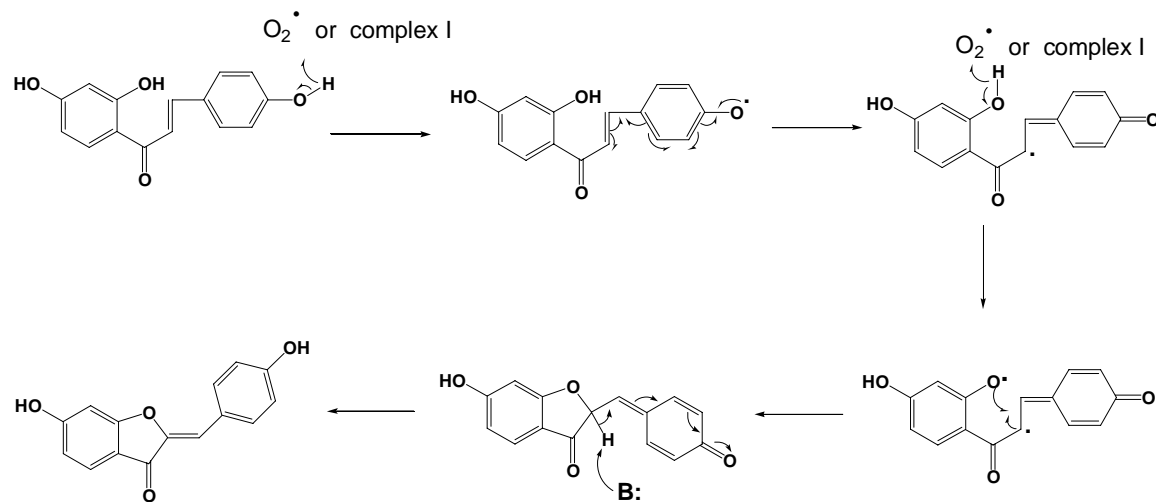


Figure 1

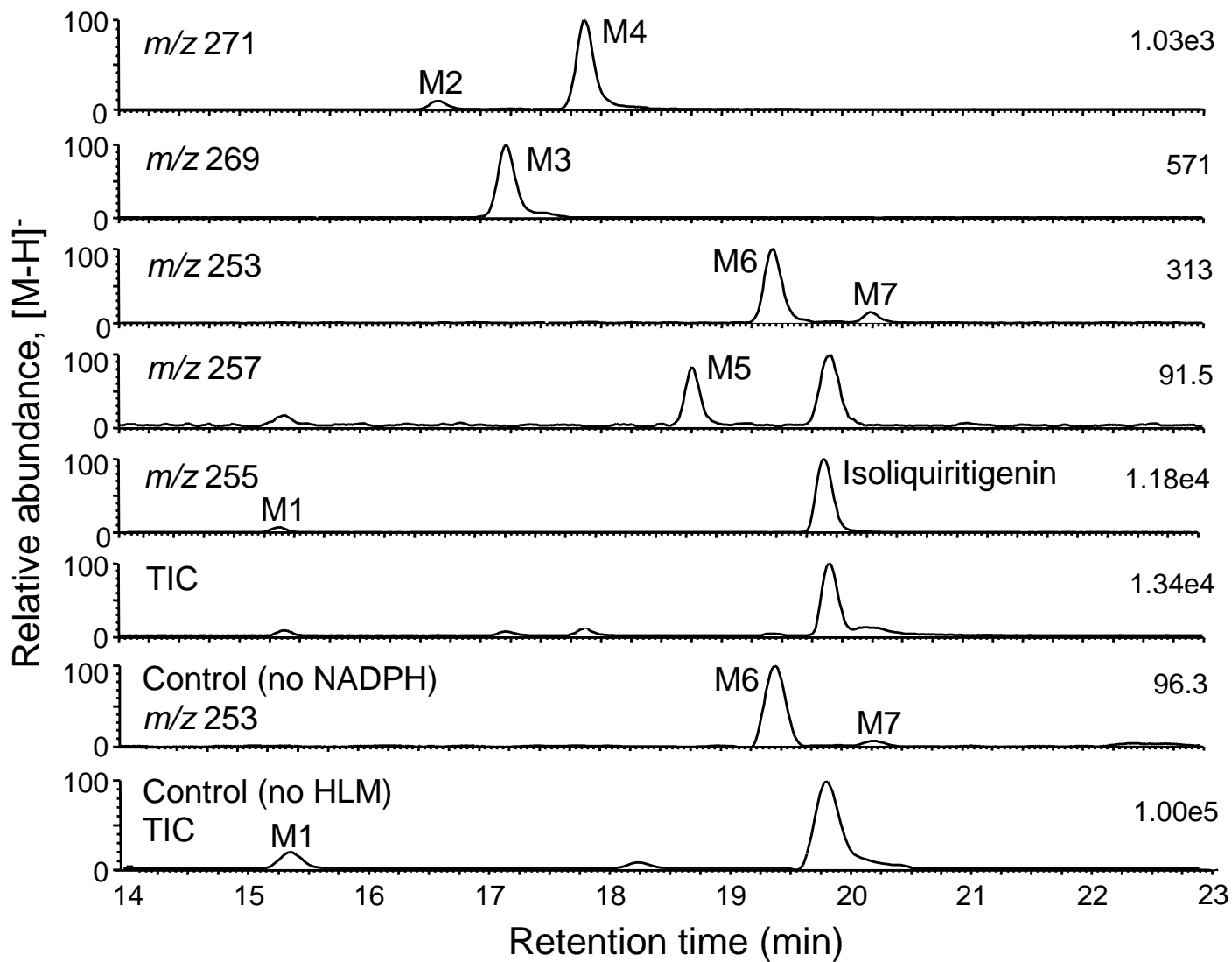


Figure 2

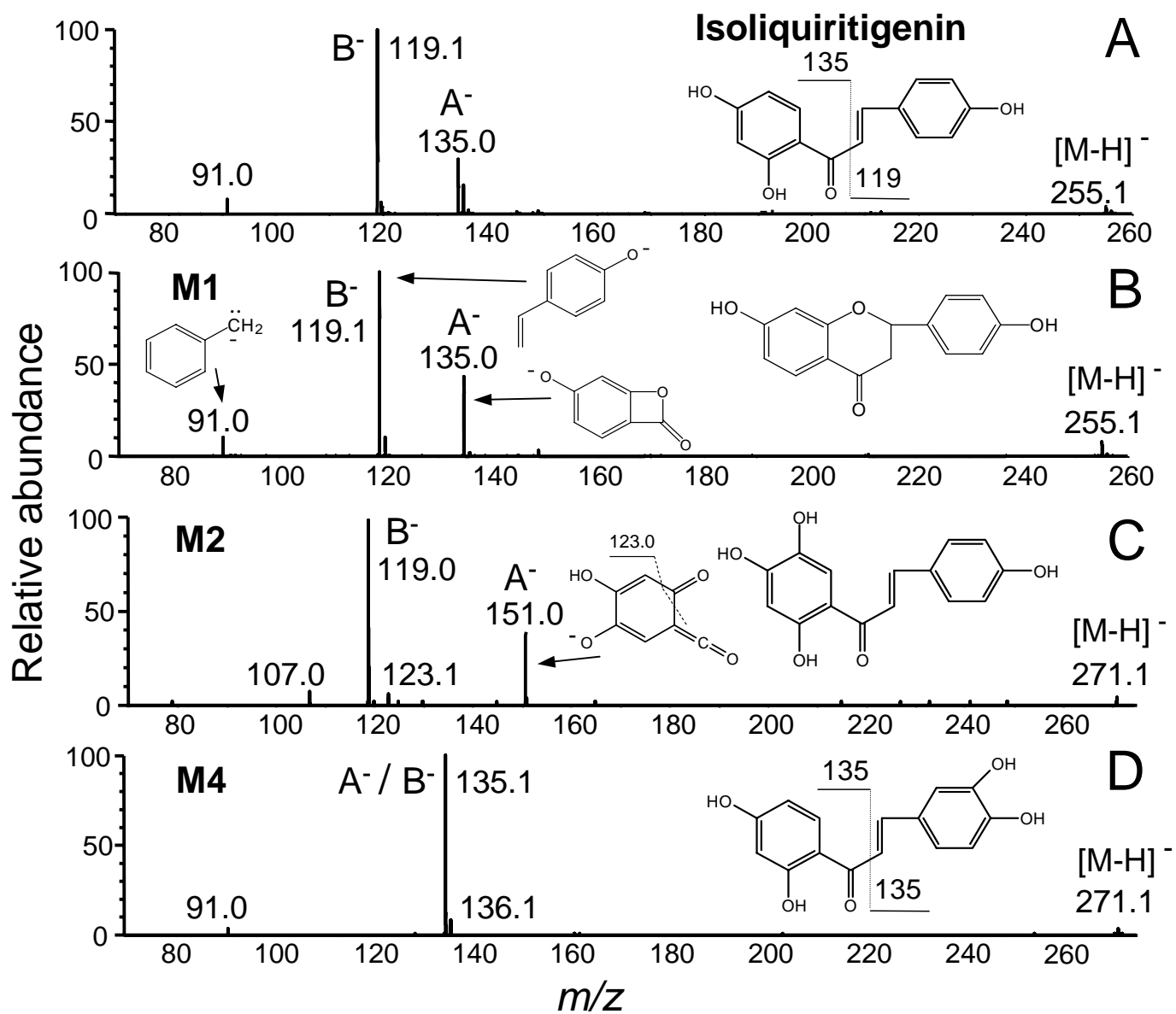


Figure 3

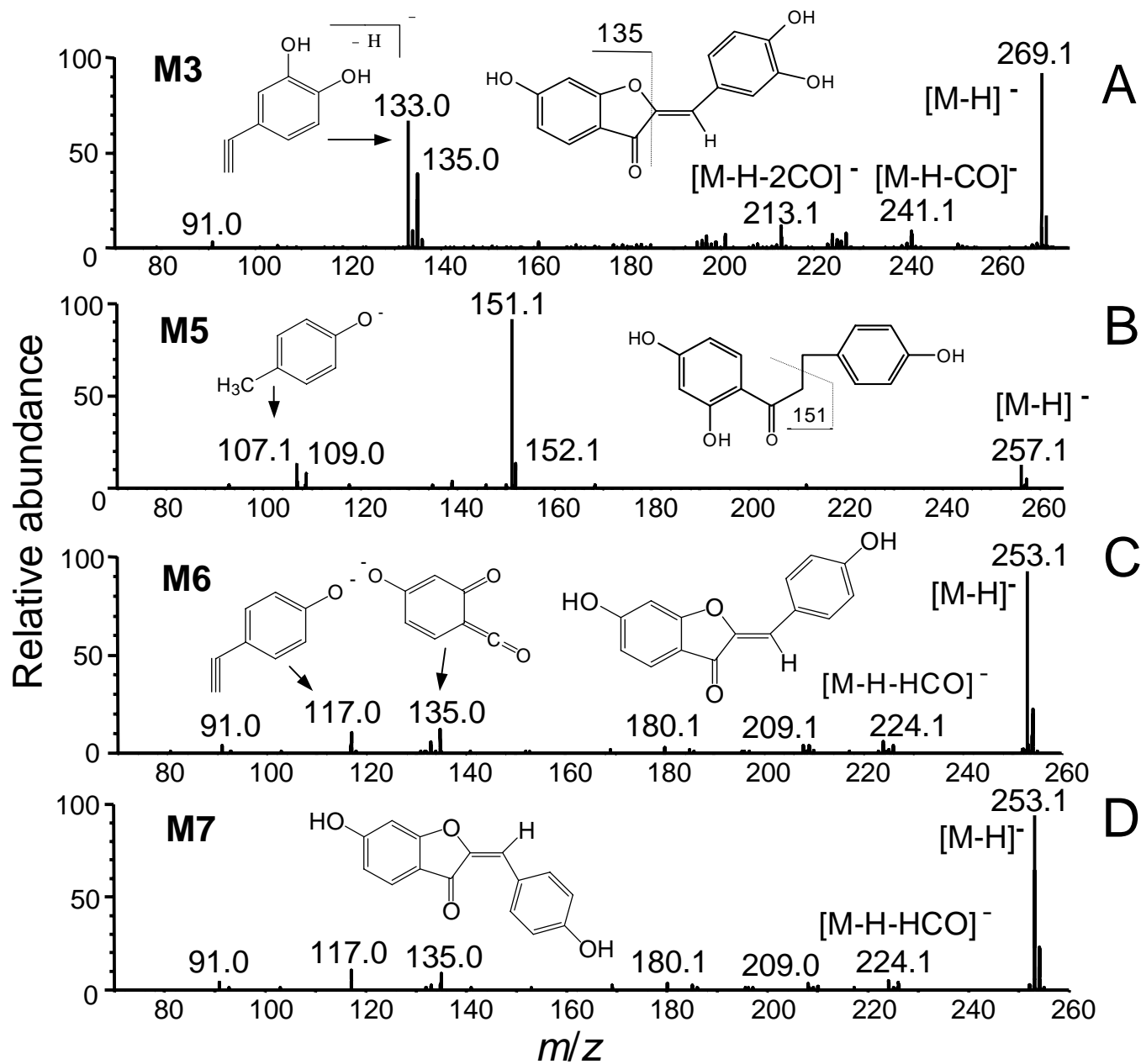


Figure 4

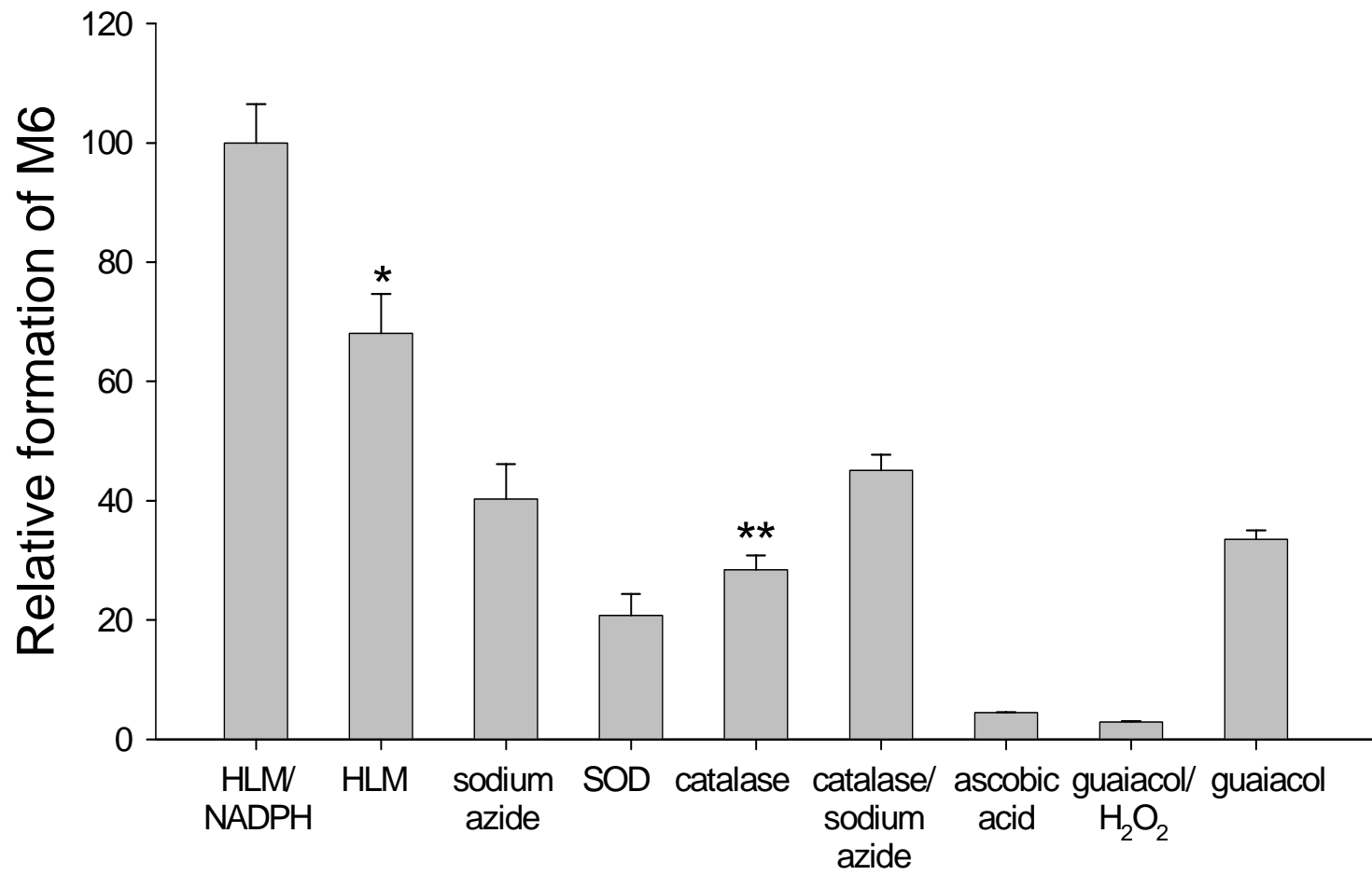


Figure 5

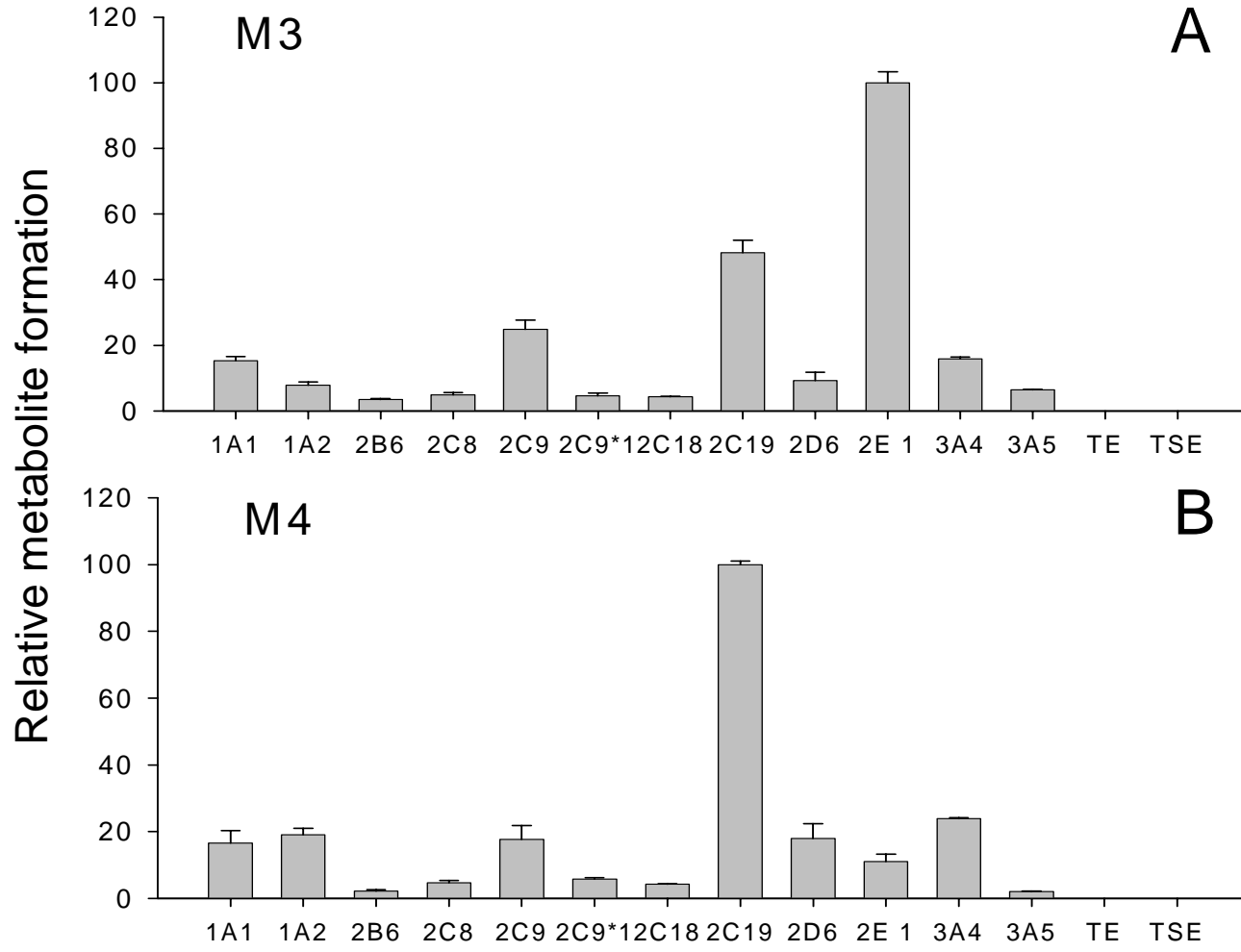


Figure 6

